

# Mechanical Properties and Chloride Diffusion of Ceramic Waste Aggregate Mortar Containing Ground Granulated Blast–Furnace Slag

H. Higashiyama, M. Sappakittipakorn, M. Mizukoshi, O. Takahashi

**Abstract**—Ceramic Waste Aggregates (CWAs) were made from electric porcelain insulator wastes supplied from an electric power company, which were crushed and ground to fine aggregate sizes. In this study, to develop the CWA mortar as an eco-efficient, ground granulated blast–furnace slag (GGBS) as a Supplementary Cementitious Material (SCM) was incorporated. The water–to–binder ratio (W/B) of the CWA mortars was varied at 0.4, 0.5, and 0.6. The cement of the CWA mortar was replaced by GGBS at 20 and 40% by volume (at about 18 and 37% by weight). Mechanical properties of compressive and splitting tensile strengths, and elastic modulus were evaluated at the age of 7, 28, and 91 days. Moreover, the chloride ingress test was carried out on the CWA mortars in a 5.0% NaCl solution for 48 weeks. The chloride diffusion was assessed by using an electron probe microanalysis (EPMA). To consider the relation of the apparent chloride diffusion coefficient and the pore size, the pore size distribution test was also performed using a mercury intrusion porosimetry at the same time with the EPMA. The compressive strength of the CWA mortars with the GGBS was higher than that without the GGBS at the age of 28 and 91 days. The resistance to the chloride ingress of the CWA mortar was effective in proportion to the GGBS replacement level.

**Keywords**—Ceramic waste aggregate, Chloride diffusion, GGBS, Pore size distribution.

## I. INTRODUCTION

CERAMIC wastes discarded worldwide from ceramic industries, demolition/construction sites, electric power companies, and railway companies are one of the materials possibly recyclable as aggregate and/or pozzolans. The utilization of the ceramic wastes has been investigated by many researchers. In the existing literature [1]–[4], however, there is a shortage on the utilization of ceramic waste aggregates (CWAs) provided from electric porcelain insulators. They have concluded that the CWAs in concrete/mortar showed no negative influence on mechanical and permeation properties. The authors [5]–[8] have also investigated on the compressive strength and the resistance to chloride ingress on the CWA

mortars. The replacement of entire fine aggregates with the CWA in mortar reduces the chloride ion penetration when compared with river sand (RS) mortar. On the other hand, it is well-known that a mineral admixture of Ground Granulated Blast–furnace Slag (GGBS) with a supplementary cementitious material (SCM) with partial cement replacement is advantage in the long-term strength gain and the resistance to weathering and aggressive chemical action. In [9], [10], the chloride ingress tests were performed on the CWA mortars partially replaced with GGBS at 15, 30, and 45% by weight. But, the water–to–binder ratio (W/B) of the CWA mortar was only 0.5. From the results [10], the GGBS significantly decreased the penetration depth of chloride ion into the CWA mortar. The changing of the apparent chloride diffusion coefficients of the CWA mortars with the GGBS was relatively small along the immersion time up to 96 weeks. Consequently, the chloride resistance of the CWA mortar was more effective with increasing the GGBS replacement level up to 45% tested.

In this study, the CWA mortars with further wide range of W/B, i.e., 0.4, 0.5, and 0.6 were investigated on the mechanical properties and the chloride ingress. The cement was partially replaced with the GGBS at 20 and 40% by volume. The mechanical tests on compressive and splitting tensile strengths were carried out at the age of 7, 28, and 91 days while the chloride ingress test was performed after 48 weeks immersion in a 5.0% NaCl solution. The chloride concentration profiles of the CWA mortars were obtained by using the electron probe microanalysis (EPMA). Furthermore, the pore size distribution in the CWA mortars was measured by using a mercury intrusion porosimetry to understand a relation with the apparent chloride diffusion coefficient.

## II. MATERIALS AND TEST METHODS

### A. Materials and Mixture Proportions

Electric porcelain insulators such as suspension porcelain insulators as shown in Fig. 1 were transferred to CWAs at a recycle plant of The Kanden L&A Company, Ltd. in Japan via the processes of crushing and grinding. After obtaining the blunt edge CWAs through these processes, the particle size ranging from 0.075 to 5.0 mm by sieving was used as fine aggregate in this study as shown in Fig. 2. The grain size distribution of the CWA with the grading requirements (dashed lines) of the standard distribution specified in JIS A 5005 [11] is presented in Fig. 3. The grain size distribution of the CWA after going through the above processes is within the standard

H. Higashiyama is an Associate Professor at the Department of Civil and Environmental Engineering, Kinki University, Higashiosaka, Osaka 577-8502 Japan (corresponding author to provide phone: +81-6-4307-3553; fax: +81-72-995-5192; e-mail: h-hirosi@civileng.kindai.ac.jp).

M. Sappakittipakorn is an Assistant Professor at the Department of Civil Engineering, King Mongkut's University of Technology North Bangkok, Bangkok, 10800 Thailand (e-mail: manote.s@eng.kmutnb.ac.th).

M. Mizukoshi is a Professor at the Department of Civil Engineering, Kagawa National College of Technology, Takamatsu, Kagawa 761-8058 Japan (e-mail: m-mizu@t.kagawa-nct.ac.jp).

O. Takahashi is a General Manager at The Kanden L&A Company, Ltd., Osaka 550-0013 Japan (e-mail: o\_takahashi@kla.co.jp).

distribution except for one particle size of 2.5 mm. The specific gravity, water absorption, and the fineness modulus of the CWA were 2.40, 0.7% by weight, and 3.20.

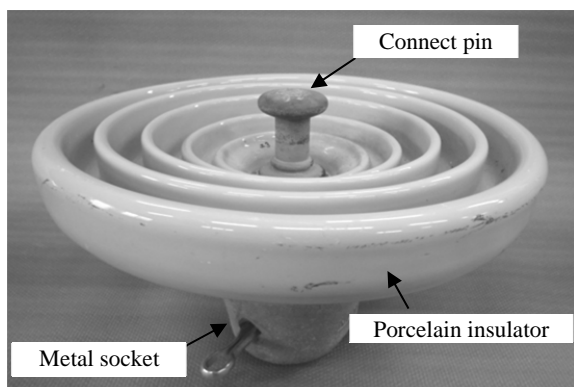


Fig. 1 Suspension porcelain insulator



Fig. 2 Ceramic waste fine aggregates

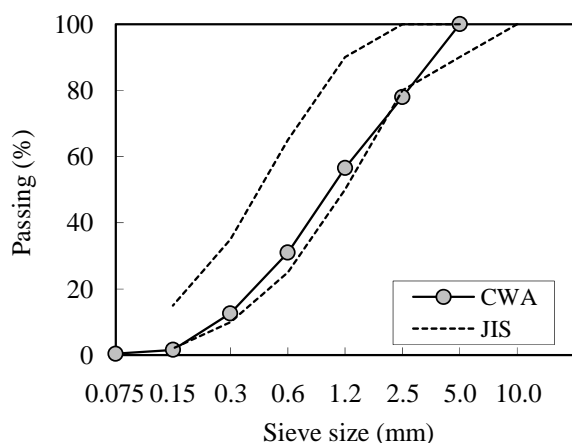


Fig. 3 Grain size distribution of CWA

The cement was ordinary Portland cement (OPC) with the specific gravity of 3.15 and the specific surface area by Blaine of 3360 cm<sup>2</sup>/g. The GGBS supplied from a slag cement company was used as a SCM in this study. The GGBS was with the specific gravity of 2.91 and the specific surface area by Blaine of 6230 cm<sup>2</sup>/g. The chemical and physical properties of

cement, GGBS, and CWA used in this study are given in Table I.

TABLE I  
CHEMICAL AND PHYSICAL PROPERTIES

Properties	Cement	GGBS	CWA
Chemical compositions (wt.%)			
SiO <sub>2</sub>	20.68	33.80	70.90
Al <sub>2</sub> O <sub>3</sub>	5.28	15.00	21.10
Fe <sub>2</sub> O <sub>3</sub>	2.91	0.27	0.81
CaO	64.25	43.10	0.76
MgO	1.40	5.63	0.24
SO <sub>3</sub>	2.10	-	-
Na <sub>2</sub> O	0.28	0.28	1.47
K <sub>2</sub> O	0.40	0.31	3.57
TiO <sub>2</sub>	0.28	0.52	0.33
P <sub>2</sub> O <sub>5</sub>	0.25	-	-
MnO	0.09	0.20	-
SrO	0.06	-	-
S	-	0.77	-
Cl	0.015	0.004	-
Loss on ignition	1.80	0.05	-
Specific gravity	3.15	2.91	2.40
Specific surface area (cm <sup>2</sup> /g)	3360	6230	-

TABLE II  
MIXTURE PROPORTION OF CWA MORTAR

Mixture	W/B (%)	Water (kg/m <sup>3</sup> )	Cement (kg/m <sup>3</sup> )	CWA (kg/m <sup>3</sup> )	GGBS (kg/m <sup>3</sup> )
CWA40-0	40.0	303	758	1095	0
CWA40-20	40.6	303	607	1095	140
CWA40-40	41.2	303	455	1095	280
CWA50-0	50.0	303	606	1211	0
CWA50-20	50.8	303	485	1211	112
CWA50-40	51.5	303	364	1211	224
CWA60-0	60.0	303	505	1288	0
CWA60-20	60.8	303	404	1288	94
CWA60-40	61.8	303	303	1288	187

In the mixture proportion of the previous study [9], [10], the CWA-to-binder ratio (S/B) of the CWA mortars with and without GGBS was simply kept constant at 2.0 by weight. In this study, however, the mixture proportion was designed by volume as presented in Table II. Accordingly, the cement in the CWA mortar was also replaced by the GGBS at 20 and 40% by volume. Therefore, the W/B was almost 0.4, 0.5, and 0.6.

### B. Specimens

For all mixtures, the CWA mortars were prepared in a Hobart mixer of 5 L capacity. The mixing process started with the blending of the OPC, GGBS and CWA for 1 min and was followed with the addition of water and further mixing for 3 min. For each mixture, eighteen cylindrical specimens of 50 mm diameter and 100 mm height were cast; nine of which were used in compression tests and the other nine were used in splitting tensile tests at the age of 7, 28, and 91 days (three specimens at each time). Furthermore, two cylindrical specimens of 100 mm diameter and 200 mm height were prepared for chloride ingress tests at 48 and 96 weeks immersion (one specimen at each time) which were employed

in EPMA. In this paper, a result of the chloride ingress test at 48 weeks immersion was reported. The specimens for 96 weeks immersion are under continuing. After casting, all specimens were covered with a plastic waterproof sheet for 24 h. Subsequently, they were demoulded and cured in a water tank at  $20 \pm 2$  °C.

### C. Test Methods

Compression and splitting tensile tests were carried out on the three specimens for each mixture at the age of 7, 28, and 91 days. In the compression test, two strain gauges were glued on a specimen to calculate the elastic modulus.

At the age of 7 days, the specimens for the chloride ingress test were cut down from 200 mm to 150 mm height with 50 mm top end discarded to eliminate the influence of segregation. After the specimens were allowed to dry in a laboratory condition at  $20 \pm 2$  °C for 24 h, they were epoxy coated leaving only one sawn surface free of coating and were kept for additional 24 h to cure the epoxy resin. Then, they were fully immersed in a 5.0% NaCl solution in hermetic tanks at  $20 \pm 2$  °C for 48 weeks until the EPMA. The NaCl solution was changed at each three months interval.

After the immersion was completed, one specimen for each mixture was followed with the EPMA. The specimens were cut into 25 mm width and 60 mm length as shown in Fig. 4. By using the JEOL JXA-8200 instrument, the resized specimens were scanned to identify the amount of chloride ions at tiny single spot throughout its surface. The measurement conditions were an accelerating voltage of 15 kV, a beam current of 0.2  $\mu$ A, a pixel size of 200  $\mu$ m, a probe diameter of 150  $\mu$ m, and the number of mapping points of  $400 \times 400$  pixels. The chloride concentration profiles were plotted and were analyzed to find the apparent chloride diffusion coefficient.

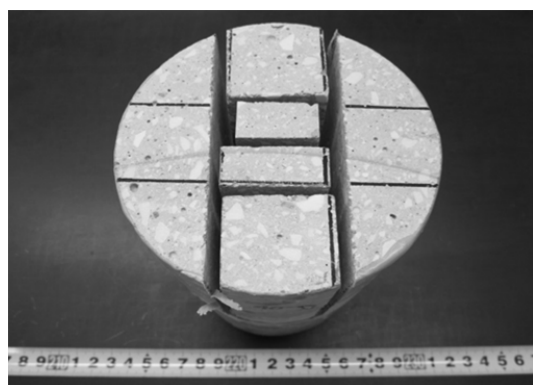


Fig. 4 Preparation of specimen for EPMA

By using the same CWA mortars of the EPMA, the test pieces with 2.5 to 5.0 mm size were obtained from the center of cylindrical specimen by crushing. The samples of 30 g were collected from them and were vacuum-dried for 24 h. The pore size distribution test was performed using a mercury intrusion porosimetry (PoreMaster 60GT, Quantachrome). For each mortar, the sample of the pore size distribution ranging from 0.007 to 200  $\mu$ m of pore diameter was measured.

TABLE III  
AVERAGED RESULTS OF MECHANICAL PROPERTIES

Mixture	Compressive strength (N/mm <sup>2</sup> )	Tensile strength (N/mm <sup>2</sup> )	Elastic modulus (kN/mm <sup>2</sup> )
CWA40-0	63.3	3.65	31.9
CWA40-20	68.0	4.20	32.1
CWA40-40	68.1	3.90	32.1
CWA50-0	48.2	3.33	28.5
CWA50-20	49.5	3.26	28.5
CWA50-40	56.1	4.13	29.8
CWA60-0	35.5	2.91	28.3
CWA60-20	41.5	3.51	29.2
CWA60-40	40.5	3.95	28.4

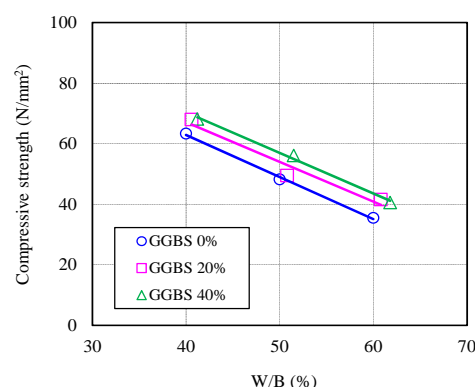


Fig. 5 Compressive strength and W/B

## III. RESULTS AND DISCUSSION

### A. Mechanical Properties

The averaged values of compressive and splitting tensile strengths and elastic modulus at the age of 28 days for all mixtures are listed in Table III. The compressive strength as a function of W/B is presented in Fig. 5. It is observed that the compressive strength was linearly increased with decreasing the W/B. From those regression lines, the compressive strength increased with the GGBS replacement level. The tensile strength and elastic modulus are presented with the compressive strength in Figs. 6 and 7, respectively. The tensile strength of the CWA mortar was increased with the compressive strength and was increased at a higher rate when the GGBS was incorporated. However, the influence of GGBS replacement level on such increase was small. The elastic modulus was also increased when the compressive strength was increased. But, there was no difference on the increasing rate between the CWA mortar with and without the GGBS.

### B. Chloride Ion Penetration Depth

By using the EPMA method, the  $25 \times 60$  mm cross sectional area of specimens was scanned to quantify the chloride concentration. The mapping result, for example, of specimens with W/B of 0.5 is shown in Fig. 8. In this figure, the upper side is the exposed surface. The chloride ion penetration depth was decreased with increasing the GGBS replacement level. The chloride concentration profiles, which were averaged along the same penetration depth at 0.2 mm intervals, are shown in Fig. 9.

It can be seen that the GGBS has great inhibiting ability against the chloride ingress. The effectiveness of GGBS as the SCM has been widely reported so far. Similarly, as reported in the previous study [9], [10], the chloride ion penetration depth becomes shorter when the W/B is lower and the GGBS replacement level is higher. This is attributed to the more refined pore structure of the hydrated cementitious material using the GGBS and the binding adsorption capacity which is chloride ion onto the hydrated slag wall [12].

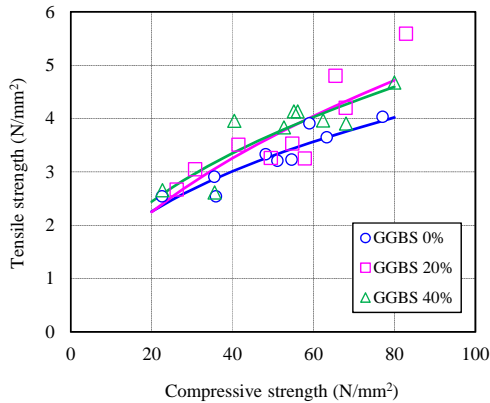


Fig. 6 Tensile strength and compressive strength

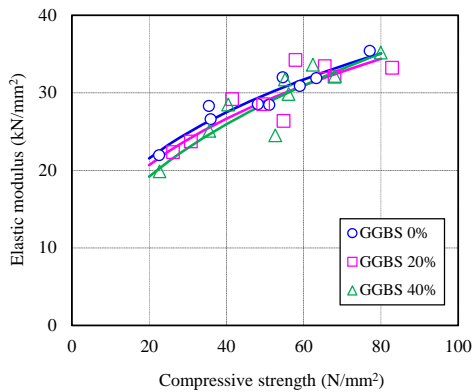


Fig. 7 Elastic modulus and compressive strength

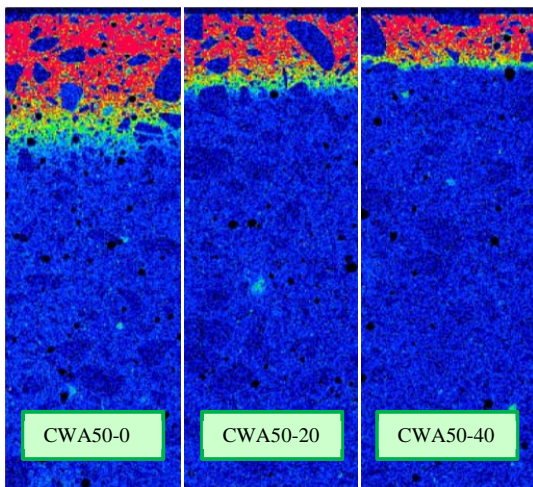
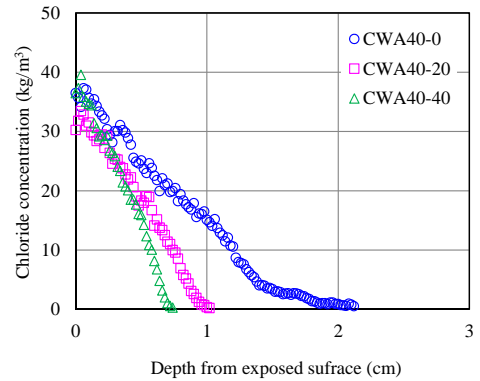
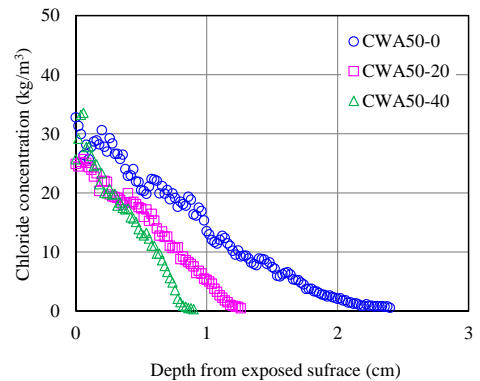


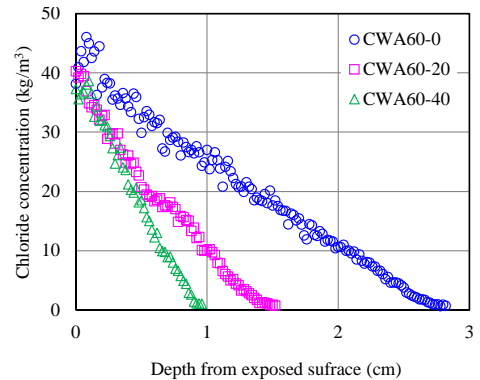
Fig. 8 Mapping results of chloride concentration



(a) W/B = 40%



(b) W/B = 50%



(c) W/B = 60%

Fig. 9 Chloride concentration profiles

### C. Apparent Chloride Diffusion Coefficient

The apparent chloride diffusion coefficient was determined by fitting the chloride concentration profile to the following Fick's second law.

$$C(x,t) = C_i + C_0 \left( 1 - \operatorname{erf} \frac{x}{2\sqrt{D_a \cdot t}} \right) \quad (1)$$

where  $C(x, t)$  is the chloride concentration ( $\text{kg/m}^3$ ) at depth  $x$  (cm) and exposure time  $t$  (year),  $C_i$  is the initial chloride concentration ( $\text{kg/m}^3$ ),  $C_0$  is the surface chloride concentration ( $\text{kg/m}^3$ ),  $D_a$  is the apparent chloride diffusion coefficient

( $\text{cm}^2/\text{year}$ ), and  $erf$  is the error function.

In the analysis of the chloride concentration profile, for the surface chloride concentration, the maximum value obtained from the result of EPMA was used and the apparent chloride diffusion coefficient was obtained by the curve fitting. The apparent chloride diffusion coefficients after analyzed are given in Table IV. Furthermore, the relation of the apparent chloride diffusion coefficient and the GGBS replacement level is shown in Fig. 10. The apparent chloride diffusion coefficient decreased with increasing the GGBS replacement level. Especially, the apparent chloride diffusion coefficient of the CWA mortar with the W/B of 60% decreased sharply when the

TABLE IV  
APPARENT CHLORIDE DIFFUSION COEFFICIENTS

Mixture	W/B (%)	GGBS replacement (vol.%)	Apparent chloride diffusion coefficient ( $\text{cm}^2/\text{year}$ )
CWA40-0	40.0	0	0.500
CWA40-20	40.6	20	0.233
CWA40-40	41.2	40	0.126
CWA50-0	50.0	0	0.700
CWA50-20	50.8	20	0.351
CWA50-40	51.5	40	0.134
CWA60-0	60.0	0	1.271
CWA60-20	60.8	20	0.333
CWA60-40	61.8	40	0.181

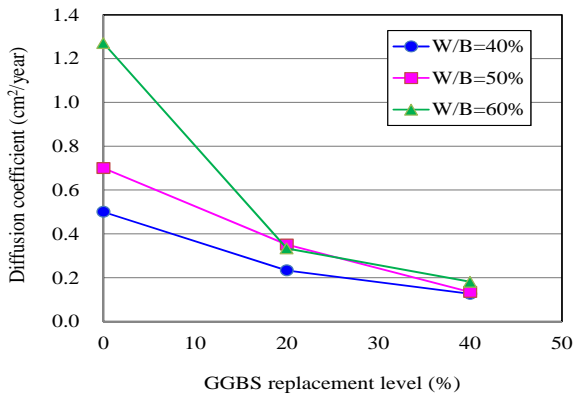


Fig. 10 Relation of apparent chloride diffusion coefficient and GGBS replacement level

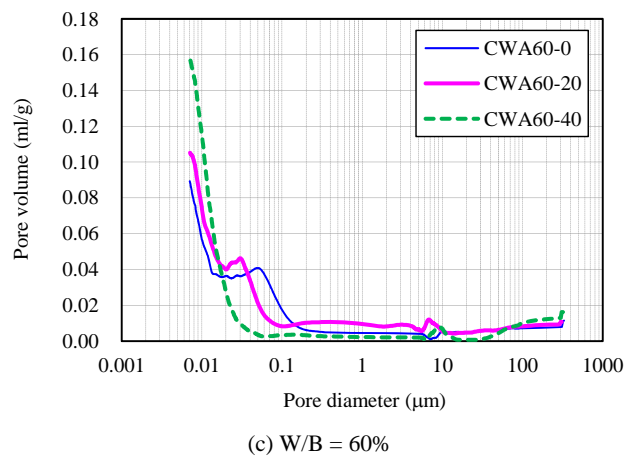
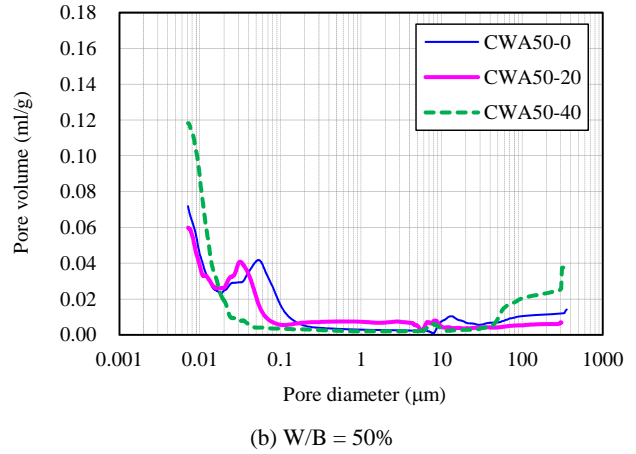
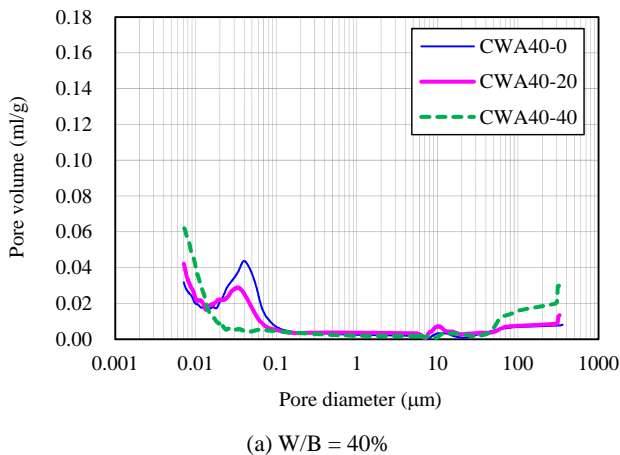


Fig. 11 Pore size distributions

GGBS was contained at 20% by volume. At the GGBS replacement level of 40%, the apparent chloride diffusion coefficient of each specimen was close.

#### D. Pore Size Distribution

The pore size distributions ranging from 0.007 to 200  $\mu\text{m}$  pore diameter are shown in Fig. 11. The pore volume was clearly decreased in the region of the smaller pore size when the W/B was lower. Furthermore, the pore size distribution was shifted to the smaller pore diameter with increasing the GGBS replacement level. One peak value of the pore volume was observed around 0.04  $\mu\text{m}$  in the CWA mortar without and with the GGBS of 20%. However, in the CWA mortar with the GGBS of 40%, no peak value exhibited and the smaller pore size less than 0.04  $\mu\text{m}$  mostly occupied the pore volume.

From the results shown in Fig. 11, the pore size distribution significantly changed in the smaller pore size less than about 0.2  $\mu\text{m}$ . In this study, the average pore volume ranging from 0.007 to 0.2  $\mu\text{m}$  pore diameter was calculated for all the specimens. Then, an exponential relation of the apparent chloride diffusion coefficient and the average pore volume can be obtained as shown in Fig. 12. Both the apparent chloride diffusion coefficient and the pore size distribution depend on the hydration of cementitious material and the binding adsorption capacity depends on the hydrated slag wall.

However, those are changed with the time. Therefore, further investigation might be needed to understand its relation shown in Fig. 12.

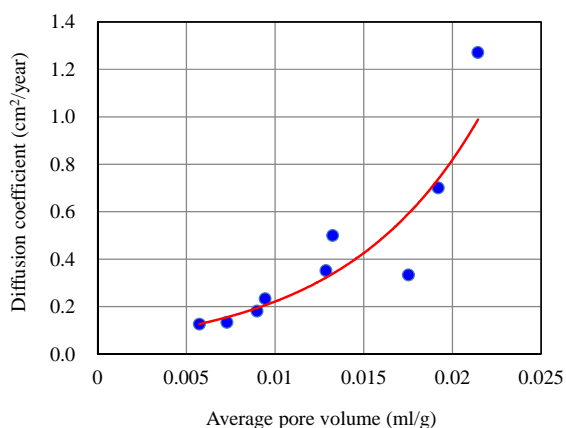


Fig. 12 Relation of apparent chloride diffusion coefficient and average pore volume

#### IV. CONCLUSIONS

In this study, the mechanical properties and chloride diffusion of the CWA mortars containing the GGBS with different W/B and replacement levels were investigated. The following conclusions can be drawn.

- (1) The compressive strength of the CWA mortar increased with increasing the GGBS replacement level. The splitting tensile strength of the CWA mortar with the GGBS increased in the region of the higher compressive strength while the influence of containing the GGBS to the elastic modulus was small.
- (2) The GGBS has great inhibiting ability against the chloride ingress. The apparent chloride diffusion coefficient decreased with increasing the GGBS replacement level. However, in the higher GGBS replacement of 40%, the difference of the apparent chloride diffusion coefficient was small within the W/B of 40 to 60% tested.
- (3) The pore volume in the region of the smaller pore size was clearly decreased by the GGBS replacement. The pore size distribution significantly changed in the smaller pore size less than about 0.2  $\mu\text{m}$ . The average pore volume ranging from 0.007 to 0.2  $\mu\text{m}$  pore diameter might be related to the apparent chloride diffusion coefficient as an exponential function.

#### ACKNOWLEDGMENT

The authors wish to acknowledge the financial support of JSPS KAKENHI (Grant Number 25420468), Japan. Furthermore, the authors are also grateful to Nippon Steel & Sumikin Cement Co., Ltd. for supplying the GGBS.

#### REFERENCES

- [1] H. Hata, A. Nakashita, T. Ohmura, and H. Itou, "Strength development of concrete containing granulated abandonment insulator," *Proceedings of Japan Concrete Institute*, vol. 26, no. 1, 2004, pp. 1683–1688.

- [2] R. M. Senthamari and P. D. Manoharan, "Concrete with ceramic waste aggregate," *Cement and Concrete Composites*, vol. 27, 2005, pp. 910–913.
- [3] R. M. Senthamari, P. D. Manoharan, and D. Gobinath, "Concrete made from ceramic industry waste: durability properties," *Construction and Building Materials*, vol. 25, 2011, pp. 2413–2419.
- [4] A. E. P. G. A. Jacintho, M. A. Campos, V. A. Paulon, G. Camarini, R. C. C. Lintz, and L. A. G. Barbosa, "The use of crushed porcelain electrical isolators as fine aggregate in mortars," *Proceedings of Concrete under Sever Conditions*, 2010, pp.1593–1600.
- [5] H. Higashiyama, F. Yagishita, M. Sano, and O. Takahashi, "Compressive strength and resistance to chloride penetration of mortars using ceramic waste as fine aggregate," *Construction and Building Materials*, vol. 26, 2012, pp. 96–101.
- [6] H. Higashiyama, M. Sappakittipakorn, M. Sano, and F. Yagishita, "Chloride ion penetration into mortar containing ceramic waste aggregate," *Construction and Building Materials*, vol. 33, 2012, pp. 48–54.
- [7] H. Higashiyama, K. Yamauchi, M. Sappakittipakorn, M. Sano, and O. Takahashi, "A visual investigation on chloride ingress into ceramic waste aggregate mortars having different water to cement ratios," *Construction and Building Materials*, vol. 40, 2013, pp. 1021–1028.
- [8] H. Higashiyama, M. Sappakittipakorn, M. Sano, O. Takahashi, and S. Tsukuma, "Characteristics of chloride ingress into mortars containing ceramic waste aggregate," *Journal of Material Cycles and Waste Management*, DOI: 10.1007/s10163-014-0264-8.
- [9] H. Higashiyama, M. Sappakittipakorn, M. Mizukoshi, and O. Takahashi, "Efficiency of ground granulated blast–furnace slag replacement in ceramic waste aggregate mortar," *Cement and Concrete Composites*, vol. 49, 2014, pp. 43–49.
- [10] H. Higashiyama, M. Sappakittipakorn, M. Mizukoshi, and O. Takahashi, "Time dependency on chloride diffusion of ceramic waste aggregate mortars containing ground granulated blast–furnace slag," *Journal of The Society of Materials Science, Japan*, to be published.
- [11] JIS A 5005, "Crushed stone and manufactured sand for concrete," *Japanese Industrial Standards*, 2010, pp. 146–148.
- [12] R. N. Swamy and A. Bouikni, "Some engineering properties of slab concrete as influenced by mix proportioning and curing," *ACI Materials Journal*, vol. 87, 1990, pp.210–220.